

# Inhibition effect of 1,1'-(pyridine-2,6-dihylbis(methylene))bis(5-methyl-1-*H*-pyrazole-3-carboxylic acid) on the corrosion of mild steel in 1 M HCl. Part A: Experimental study

M. El Azzouzi,<sup>1</sup> A. Aouniti,<sup>1</sup> M. El Massaoudi,<sup>2</sup> S. Radi,<sup>2</sup> B. Hammouti,<sup>1\*</sup>  
M.A. Quraishi,<sup>3</sup> H. Bendaif<sup>4</sup> and Y. El Ouadi<sup>1\*</sup>

<sup>1</sup>*Laboratoire de Chimie Analytique Appliquée Matériaux et Environnement (LCA2ME), Faculté des Sciences, University Mohammed Premier, B.P. 717, 60000 Oujda, Morocco*

<sup>2</sup>*Laboratory of Applied Chemistry and Environment (LCAE-URAC18), COSTE, Faculty of Science, University Mohammed Premier, Oujda, Morocco*

<sup>3</sup>*Center for Research Excellence in Corrosion, Research Institute (King Fahd University of Petroleum & Minerals), Dhahran, Saudi Arabia*

<sup>4</sup>*Laboratoire de Chimie Organique Macromoléculaire et produits Naturels (URAC25), Faculté des Sciences, University Mohammed Premier, 60000 Oujda, Morocco*

\*E-mail: [hammoutib@gmail.com](mailto:hammoutib@gmail.com), [y.elouadi@ump.ac.ma](mailto:y.elouadi@ump.ac.ma)

## Abstract

The inhibitory effect of 1,1'-(pyridine-2,6-dihylbis(methylene))bis(5-methyl-1-*H*-pyrazole-3-carboxylic acid) (EM1) was estimated on the corrosion of mild steel in 1 M hydrochloric acid using weight loss, Electrochemical Impedance Spectroscopy (EIS) and Tafel polarization curves. Inhibition was found to increase with increasing concentration of inhibitor studied. The adsorption of inhibitor molecules on mild steel surface was found to be spontaneous and obeyed the Langmuir adsorption isotherm. Values of inhibition efficiency calculated from weight loss, Tafel polarization curves, and EIS are in good agreement. Polarization curves showed that EM1 behaves as mixed type inhibitor in 1 M HCl medium. The results obtained showed that EM1 could serve as an effective inhibitor of the corrosion of mild steel in hydrochloric acid solution.

**Keywords:** *corrosion, inhibition, mild steel, electrochemical system, hydrochloric acid.*

Received: October 25, 2017. Published: November 7, 2017.

doi: [10.17675/2305-6894-2017-6-4-6](https://doi.org/10.17675/2305-6894-2017-6-4-6)

## 1. Introduction

The use of inhibitors is one of the most practical methods to secure metals against acid corrosion. Hydrochloric acid is produced in large quantities in Morocco. It is usually used in industries. The inhibited hydrochloric acid reduces the risk of corrosion of metals and promote adhesion of the paint to the surface treated. Moreover, these various products are also used for cleaning metal.

The presence of organic molecules in the corrosive medium retards the attack of acid on metals by adsorbing at the metal–solution interface. The modes of adsorption depend mainly on the chemical structure of the inhibitor, the chemical composition of the solution, the nature of the metal surface and the electrochemical potential of the metal–solution interface. The inhibition generally occurs by the formation of a barrier film on the metal surface leading to the decreasing reactivity of the cathodic and/or anodic sites [1].

The use of organic compounds containing oxygen, sulphur and nitrogen to reduce corrosion attack on steel has been studied in some details [2].

In order to search for new corrosion inhibitors in various acid media, our laboratory has published several works [3–7].

In this paper, the corrosion behavior of mild steel in hydrochloric acid has been studied by weight loss, potentiodynamic polarization and electrochemical impedance spectroscopy methods.

## 2. Experimental

### 2.1. Inhibitor

1,1'-(Pyridine-2,6-dihylbis(methylene))bis(5-methyl-1-*H*-pyrazole-3-carboxylic acid) was dissolved in the blank medium 1 M HCl ranging the concentrations from  $10^{-3}$  M to  $10^{-6}$  M. Figure 1 shows the molecular structure used.

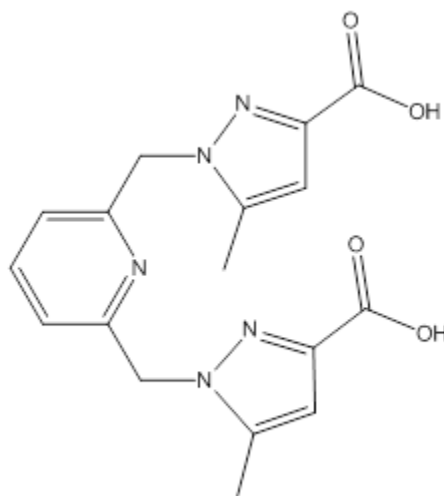


**Figure 1.** 1,1'-(Pyridine-2,6-dihylbis(methylene))bis(5-methyl-1-*H*-pyrazole-3-carboxylic acid) EM1.

### 2.2. Materials

Tests were performed on a mild steel (MS) of the following composition (0.09% P; 0.38% Si; 0.01% Al; 0.05% Mn; 0.21% C; 0.05% S and the remainder iron) were polished with emery paper up to 1200 grade, washed thoroughly with double-distilled water, degreased

with AR grade ethanol, acetone and dried at room temperature. MS samples of size  $1.0 \times 1.0 \times 1.0$  cm and MS powder were used for weight loss studies. For electrochemical studies, specimens with an exposed area of  $1 \text{ cm}^2$  were used. These specimens were degreased ultrasonically with 2-propanol and polished mechanically with different grades of emery paper to obtain very smooth surface.

### 2.3. Solution

The aggressive solutions, 1 M HCl were prepared by dilution of AR grade 37% HCl with distilled water. For pH studies, the test solutions were prepared by the dilution of distilled water up to the optimum concentration where it can reach by adjusting the pH using HCl and NaOH. Inhibitor was dissolved in acid solution at required concentrations in (mol/l) and the solution in the absence of inhibitor was taken as blank for comparison purposes. The test solutions were freshly prepared before each experiment by adding 1,1'-(pyridine-2,6-dihylbis(methylene))bis(5-methyl-1-*H*-pyrazole-3-carboxylic acid) directly to the corrosive solution. Experiments were conducted on several occasions to ensure reproducibility. Concentrations of 1,1'-(pyridine-2,6-dihylbis(methylene))bis(5-methyl-1-*H*-pyrazole-3-carboxylic acid) were  $10^{-6}$ ,  $10^{-5}$ ,  $10^{-4}$  and  $10^{-3}$  mol/l.

### 2.4. Weight loss measurements

The weight loss was employed as the principal measure of corrosion. Use of weight loss as a measure of corrosion requires making the assumption that all weight loss has been due to generalized corrosion and not localized pitting. Although these tests are simple, there is no simple way to extrapolate the results to predict the lifetime of the system under investigation. Moreover, some corrosion processes occur with no significant mass change (e.g. pitting corrosion) making them difficult to detect by gravimetric method [8]. The simplest way of measuring the corrosion rate of a metal is to expose the sample to the test medium (e.g. sea water) and measure the loss of weight of the material as a function of time. The gravimetric test is based on the immersion of the steel plates in iron, in 100 ml of a 1 M HCl solution containing the inhibitor studied at different concentrations, after be degreased, polished and weighed. Immersion is subjected to a temperature of 308 K to 6 hours.

### 2.5. Electrochemical measurements

The corrosion phenomena is electrochemical nature and consist of reactions on the surface of the corroding metal. Therefore, electrochemical tests methods can be used to characterize corrosion mechanisms and predict corrosion rates.

#### 2.5.1. Potentiodynamic polarization

This potentiostat was connected to a conventional three-electrode cell assembly. A saturated calomel electrode (SCE) and platinum electrode were used as reference and

auxiliary electrodes respectively. The material used for constructing the working electrode was the same used for gravimetric measurements. The working electrode is in the form of a rectangular disk from carbon steel of the surface  $0.32 \text{ cm}^2$ . These electrodes are connected to Voltalab PGZ 301 piloted by ordinate associated to “Volta Master 4” software. The scan rate was  $1 \text{ mV/s}$  started from an initial potential of  $-800$  to  $-200 \text{ mV/SCE}$ . All experiments were repeated three times at the desired temperature of  $\pm 274 \text{ K}$ . Corrosion current densities were obtained from the polarization curves by linear extrapolation of the Tafel curves. Prior to the electrochemical measurement, a stabilization period of  $30 \text{ min}$  was allowed, which was proved to be sufficient to attain a stable value of corrosion potential ( $E_{\text{corr}}$ ). Tafel polarization curves were plotted at a polarization scan rate of  $1 \text{ mV/s}$ . Anodic and cathodic curve slopes were extrapolated to corrosion potential, for the determination of the corrosion current densities ( $I_{\text{corr}}$ ). The Tafel equations predict a straight line for the variation of the logarithm of current density with potential. Therefore, currents are often shown in semi logarithmic plots known as Tafel plots. This type of analysis is referred to as Tafel Slope Analysis. The Tafel slope analysis tool provides a quick estimation of the corrosion rate and the polarization resistance. The corrosion rate is calculated from the estimated corrosion current,  $I_{\text{corr}}$ , obtained from the intercept of the two linear segment of the Tafel slope.

### 2.5.2. Electrochemical impedance spectroscopy

Electrochemical Impedance Spectroscopy (EIS) has many advantages in comparison with other electrochemical techniques. During EIS experiments, a small amplitude ac signal is applied to the system being studied. Therefore, it is a non-destructive method for the evaluation of a wide range of materials, including coatings, anodized films and corrosion inhibitors. It can also provide detailed information of the systems under examination; parameters such as corrosion rate, electrochemical mechanisms and reaction kinetics, detection of localized corrosion, can all be determined from these data. Electrochemical impedance spectroscopy (EIS) was carried out with the same equipment used for the polarization measurements, leaving the frequency response analyzer out of consideration. Quasi-potentiostatic polarization curves were obtained using a sweep rate of  $1 \text{ mV/s}$ . After the determination of steady-state current at a given potential, sine wave voltage ( $10 \text{ mV}$ ) peak to peak, at frequencies between  $100 \text{ kHz}$  and  $10 \text{ mHz}$  was superimposed on the rest potential. Computer programs automatically controlled the measurements performed at rest potential after  $30 \text{ min}$  of exposure. All potentials were reported *versus* saturated calomel electrode (SCE). The impedance diagrams are given in the Nyquist representation. Experiments are repeated three times to ensure the reproducibility. All electrochemical studies were carried out with immersion time of  $1 \text{ hour}$ , with different inhibitory concentrations of 1,1'-(pyridine-2,6-dihylbis(methylene))bis(5-methyl-1-*H*-pyrazole-3-carboxylic acid), at  $308 \text{ K}$ .

### 3. Results and discussion

#### 3.1. Weight loss measurements

The gravimetric method (weight loss) is known to be the most widely used method of monitoring inhibition efficiency [9]. The mild steel specimens of dimension  $1 \times 1 \times 0.1$  cm were used in these studies. The weight loss measurements were conducted under total immersion using 250 mL capacity beakers containing 100 mL of test solutions, 1 M HCl solution containing the inhibitor (1,1'-(pyridine-2,6-dihylbis(methylene))bis(5-methyl-1-*H*-pyrazole-3-carboxylic acid)) at different concentrations, for 6 hours, maintained in a thermostated water bath. Immersion is subjected to a temperature of 308 K to 6 hours. The specimens were weighed before and after the tests using an analytical balance with a precision of 0.1 mg. The specimens were taken out after the 6 hours of immersion, washed, dried and reweighed accurately to determine the weight loss of mild steel. All measurements were performed few times and average values were reported to obtain good reproducibility. The corrosion rate ( $C_R$ ) in  $\text{mg cm}^{-2} \text{h}^{-1}$  in the absence and presence of 1,1'-(pyridine-2,6-dihylbis(methylene))bis(5-methyl-1-*H*-pyrazole-3-carboxylic acid) was determined using the following equation:

$$C_R = \frac{\Delta W}{At} \quad (1)$$

where  $\Delta W$  is the average weight loss of the mild steel specimens,  $A$  is the total area of mild steel specimen and  $t$  is the immersion time. The percentage inhibition efficiency ( $I_E$  %) was calculated using the relationship:

$$I_E(\%) = \frac{W_0 - W_i}{W_0} \times 100 \quad (2)$$

where  $W_0$  and  $W_i$  are the weight loss values in the absence and presence of 1,1'-(pyridine-2,6-dihylbis(methylene))bis(5-methyl-1-*H*-pyrazole-3-carboxylic acid).

Table 1 listed the corrosion rate values and the efficiencies of the inhibitions for each concentration, it is clear that 1,1'-(pyridine-2,6-dihylbis(methylene))bis(5-methyl-1-*H*-pyrazole-3-carboxylic acid) showed a best inhibitive effect, the efficiency reach until 93% in HCl 1 M medium at  $10^{-3}$  mol/l. This result could be explain by the fact that the adsorption coverage increases with the increase of inhibitor's concentration, which shields the mild steel surface efficiently from the medium [5].

**Table 1.** Weight loss measurements of different concentration with and without presence of inhibitor (EM1) in 1 M HCl medium.

Compound	Concentration (M)	Corrosion rate (mg/cm <sup>2</sup> ·h)	Efficiency (%)
Blank	1	0.8270	–
EM1	1.10 <sup>-3</sup>	0.0572	<b>93</b>
	1.10 <sup>-4</sup>	0.0960	88
	1.10 <sup>-5</sup>	0.1426	82
	1.10 <sup>-6</sup>	0.2612	68

### 3.2. Adsorption isotherm

Metal surface providing us several information about the adsorption mechanism of the inhibitors on the surface by studying the relationship between the concentration and the surface coverage. Many isotherms are employed to fit the experimental data such as Langmuir, Temkin, Frumkin, *etc.*

It is found that the adsorption of studied inhibitor on steel surface obeys the Langmuir adsorption isotherm equation:

$$\frac{C}{\theta} = \frac{1}{K} + C \quad (3)$$

where  $C$  is the concentration of inhibitor,  $K$  the adsorption equilibrium constant, and  $\theta$  is the surface coverage.

Plots of  $C/\theta$  against  $C$  yield straight lines as shown in Figure 2, and the corresponding linear regression parameters are listed in Table 2. Both linear correlation coefficient ( $r$ ) and slope are close to 1, indicating the adsorption of (EM1) inhibitor on mild steel surface obeys Langmuir adsorption isotherm.

Furthermore, the adsorption equilibrium constant ( $K$ ) is related to the standard free energy  $\Delta G^0$  by the following equation:

$$\Delta G_{\text{ads}}^0 = -RT \cdot \ln(55.5 \cdot K) \quad (4)$$

where  $R$  is the gas constant (8.314 J K<sup>-1</sup> mol<sup>-1</sup>),  $T$  the absolute temperature (K), and the value 55.5 is the concentration of water in the solution.

Table 2 represents the  $\Delta G_{\text{ads}}^0$  values, the negative values of the free energy means that the inhibitor was spontaneously adsorbed on mild steel–electrolyte interface. It has been reported that values of  $\Delta G_{\text{ads}}^0$  up to –20 kJ/mol are consistent with the physisorption; those around –40 kJ/mol or higher are consistent with chemisorptions [10]. In the present study, the value of  $\Delta G_{\text{ads}}^0$  is found to be around –43 kJ mol<sup>-1</sup>, probably means that the adsorption of the inhibitor on the steel surface exhibits chemical adsorption.

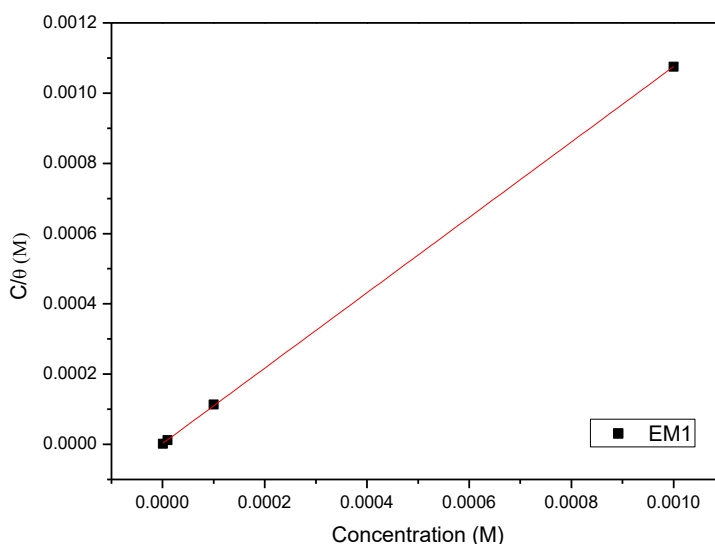


**Figure 2.** Langmuir adsorption of (EM1) on the mild steel in 1 M HCl medium.

**Table 2.** Thermodynamics parameters of (EM1) adsorption on the mild steel in 1 M HCl media.

Compound	Linear correlation	Slope	$K$	$\Delta G^0$ (kJ mol <sup>-1</sup> )
EM1	0.9999	1.0731	$4.15 \cdot 10^4$	-43.409

### 3.3. Electrochemical impedance measurements

The EIS is a method designed to avoid severe deterioration of the exposed surface of the structure studied and was widely used for monitoring the corrosion of a working electrode. This method consists of applying frequencies and low amplitude sinusoidal voltage wave to produce perturbation signals on the working electrode. The corrosion state can be predicted by analyzing the current response of the voltage or the frequencies. In modern practice, the impedance is usually measured with lock-in amplifiers or frequency-response analyzers, which are faster and more convenient than impedance bridges [11].

The electrochemical cell was Pyrex of cylinder closed by cap containing five openings. Three of them were used for the electrodes. The working electrode was mild steel with the surface area of 1 cm<sup>2</sup>. Before each experiment, the electrode was polished using emery paper until 1200 grade. After this, the electrode was cleaned ultrasonically with distillate water. A saturated calomel electrode (SCE) was used as a reference. All potentials were given with reference to this electrode. The counter electrode was a platinum plate of surface area of 1 cm<sup>2</sup>. The temperature was thermostatically controlled at 308 K. The working electrode was immersed in test solution during 30 minutes until a

steady state open circuit potential ( $E_{ocp}$ ) was obtained. The polarization curve was recorded by polarization from  $-800$  mV to  $-200$  mV under potentiodynamic conditions corresponding to  $1$  mV/s (sweep rate) and under air atmosphere.

The potentiodynamic measurements were carried out using VoltaLab 301 electrochemical analyzer, which was controlled by a personal computer. AC impedance studies also were carried out in a three electrode cell assembly. The data were analyzed using Voltmaster 4.0 software. The electrochemical impedance spectra (EIS) were acquired in the frequency range  $100$  kHz to  $10$  mHz at the free corrosion potential. The charge transfer resistance ( $R_{ct}$ ) and double layer capacitance ( $C_{dl}$ ) were determined from Nyquist plots. Experiments are repeated three times to ensure the reproducibility. All electrochemical studies were carried out with immersion time of  $1$  hour, with different concentrations of  $1,1'$ -(pyridine-2,6-dihylbis(methylene))bis(5-methyl-1-*H*-pyrazole-3-carboxylic acid), at  $308$  K.

### 3.3.1. Electrochemical impedance measurements

EIS was carried out on a newly polished steel surface in acidic solution in the absence and presence of inhibitor at an open circuit potential at  $308$  K after  $30$  min of immersion.

The locus of the Nyquist plots was regarded as one part of a semicircle. Nyquist plots of steel in inhibited and uninhibited acidic solution containing various concentrations of inhibitor studied (EM1) are shown respectively in Figure 3.

The impedance diagrams obtained are not perfect semicircles and this difference has been attributed to frequency dispersion [12]. It is noteworthy that the best fit of the experimental data was obtained using constant phase elements (CPE) which have frequency dispersion rather than capacitances. Based on the values of the electric elements and parameters obtained in them, capacitances were assessed in accordance. CPE is a generalized tool, which can reflect exponential distribution of the parameters of the electrochemical reaction related to energetic barrier at charge and mass transfer, as well as impedance behavior caused by fractal surface structure. On the other hand there are some cases where the CPE is a formal approximation of the system, having very complicated parameter distribution and it is not possible to give some consistent physical interpretation. The dispersion of the capacitive semicircle is explained also by surface heterogeneity due to surface roughness, impurities or dislocations [12, 13].

The charge transfer resistance,  $R_t$  values are calculated from the difference in impedance at lower and higher frequencies, as suggested by Tsuru *et al.* [14]. To obtain the double layer capacitance ( $C_{dl}$ ), the frequency at which the imaginary component of the impedance is maximum ( $-Z_{max}$ ) is found and  $C_{dl}$  values are obtained from the equation:

$$C_{dl} = \frac{1}{2\pi f_{max} R_{ct}} \quad (6)$$

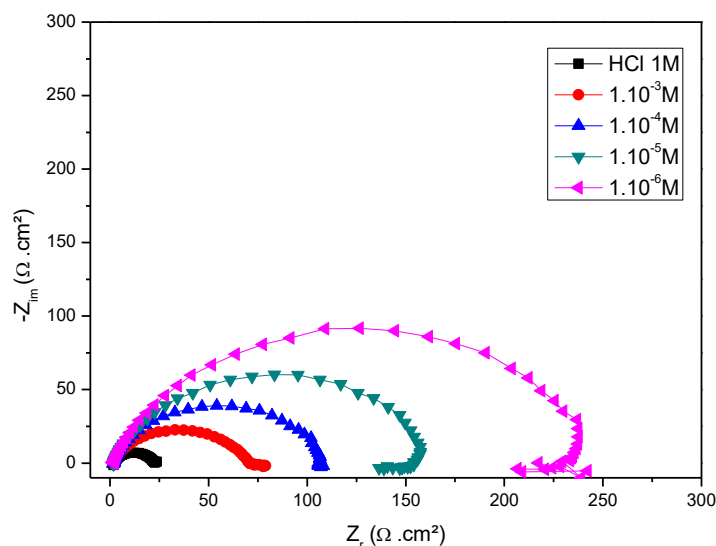


**Figure 3.** Nyquist plots of (EM1) in absence and presence of different concentrations in 1 M HCl.

The percentage inhibition efficiency from the charge transfer resistance is calculated by the following relation:

$$E(\%) = \frac{R_{ct}^0 - R_{ct}}{R_{ct}} \times 100 \quad (7)$$

where  $R_{ct}^0$  and  $R_{ct}$  are the charge transfer resistance in presence and in absence of inhibitor, respectively.

The impedance parameters derived from these investigations are given in Table 3. It is found that  $R_{ct}$  values increase with the increase in (EM1) concentrations indicating formation of an insulated film on the metal surface.

The double layer capacitance  $C_{dl}$  is expressed in the Helmutz model by:

$$C_{dl} = \frac{\epsilon_0 \epsilon}{\delta} S \quad (8)$$

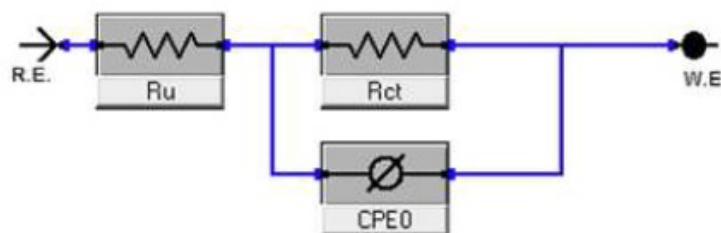
where  $\delta$  is the thickness of the deposit,  $S$  is the surface of the electrode,  $\epsilon_0$  is the permittivity of the air and  $\epsilon$  is the medium dielectric constant. The decrease in  $C_{dl}$  values may be interpreted either by a decrease of local dielectric constant  $\epsilon$  [15] or by the thickness of the adsorbate layer of inhibitor at the metal surface [16].

**Table 3.** Corrosion parameters obtained by impedance measurements for mild steel in 1 M HCl at various concentrations of (EM1).

Compound	Concentration (mol/l)	$R_{ct}$ ( $\Omega \cdot \text{cm}^2$ )	$C_{dl}$ ( $\mu\text{F} \cdot \text{cm}^{-2}$ )	Efficiency (%)
Blank	1	20.7	191.7	–
EM1	$10^{-3}$	236.5	53.86	<b>91</b>
	$5 \cdot 10^{-4}$	153.6	82.93	86
	$10^{-4}$	105.3	84.71	80
	$5 \cdot 10^{-5}$	69.2	115.05	70

From Table 3, it is clear that the  $R_{ct}$  values increased and that the  $C_{dl}$  values decreased with increasing inhibitor concentrations. These results indicate a decrease in the active surface area caused by the adsorption of the inhibitor on the mild steel surface, and it suggests that the corrosion process became hindered. The best result for the inhibition efficiency of the 1,1'-(pyridine-2,6-dihylbis(methylene))bis(5-methyl-1-*H*-pyrazole-3-carboxylic acid) was obtained at a concentration of  $10^{-3}$  mol/l, with efficiency equal to 91%.

The EIS results of these capacitive loops are simulated by the equivalent circuit shown in Figure 4 to pure electric models that could verify or rule out mechanistic models and enable the calculation of numerical values corresponding to the physical and/or chemical properties of the electrochemical system under investigation. In the electrical equivalent circuit,  $R_s$  is the electrolyte resistance,  $R_{ct}$  the charge transfer resistance and  $C_{dl}$  is the double layer capacitance.

**Figure 4.** Electrical equivalent circuit model used for the modeling metal/solution.

### 3.3.2. Polarization measurements

The polarization curves of steel in 1 M HCl in the absence and presence of 1,1'-(pyridine-2,6-dihylbis(methylene))bis(5-methyl-1-*H*-pyrazole-3-carboxylic acid) at different concentrations at 308 K are presented in Figure 5. The collected parameters deduced from the polarization curves such as the corrosion potential ( $E_{corr}$ ), corrosion current density ( $i_{corr}$ ), cathodic Tafel slopes ( $\beta_c$ ) and percentage inhibition efficiency ( $E_I$  %) are shown in Table 4. The relation determines the inhibition efficiency ( $E_I$  %):

$$E(\%) = \frac{i_{\text{corr}}^0 - i_{\text{corr}}}{i_{\text{corr}}^0} \times 100 \quad (9)$$

where  $i_{\text{corr}}^0$  and  $i_{\text{corr}}$  are uninhibited and inhibited corrosion current densities, respectively. Under the experimental conditions performed, the cathodic branch represents the hydrogen evolution reaction, while the anodic branch represents the iron dissolution reaction.

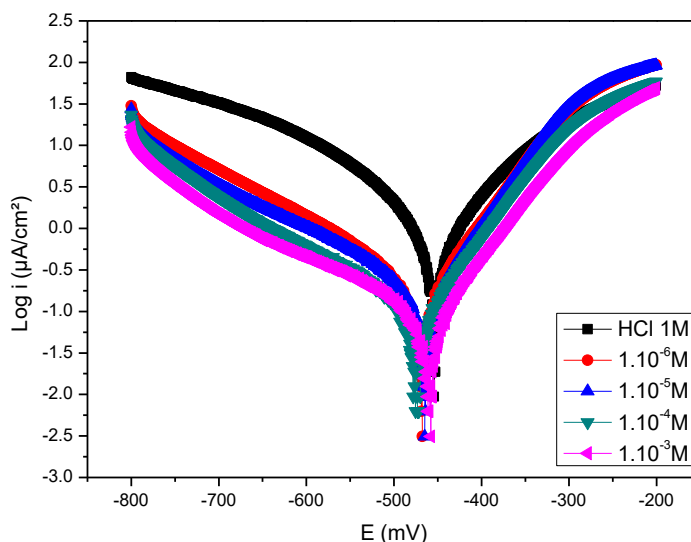


**Figure 5.** Tafel polarization curves in 1 M HCl with and without (EM1) at different concentrations.

**Table 4.** Corrosion parameters obtained by electrochemical Tafel Polarization method measurements for mild steel in 1 M HCl at various concentrations of (EM1).

Compound	Conc. (mol/l)	$E_{\text{corr}}$ (mV vs. SCE)	$i_{\text{corr}}$ (mA/cm <sup>2</sup> )	$\beta_c$ (mV)	$\beta_a$ (mV)	Efficiency (%)
Blank	1	-454	1.9477	-182.9	151.8	–
EM1	$1 \cdot 10^{-3}$	-460	0.0680	-184.1	73.0	<b>96</b>
	$1 \cdot 10^{-4}$	-473	0.0787	-153.5	72.3	94
	$1 \cdot 10^{-5}$	-465	0.2267	-206.2	80.1	88
	$1 \cdot 10^{-6}$	-469	0.2678	-181.0	83.3	86

Generally, the modes of the inhibition effect of inhibitors are classified into three categories [17]: geometric blocking effect of adsorbed inhibitive species, active sites blocking effect by adsorbed inhibitive species, and electro catalytic effect of the inhibitor

or its reaction products. It has been discussed in the case of the first mode that inhibition effect comes from the reduction of the reaction area on the surface of the corroding metal, whereas for the other two modes the inhibition effects are due to the changes in the average activation energy barriers of the anodic and cathodic reactions of the corrosion process. The cathodic Tafel slope ( $\beta_c$ ) show slight changes with the addition of (EM1), which suggests that the inhibiting action occurred by simple blocking of the available cathodic sites on the metal surface, which lead to a decrease in the exposed area necessary for hydrogen evolution and lowered the dissolution rate with increasing inhibitor concentration. From Table 4, it is clear that increasing concentration of the inhibitor (EM1) resulted in a decrease in corrosion current densities ( $i_{\text{corr}}$ ) and an increase in inhibition efficiency (IE %), reaching its maximum value, 96%, at  $10^{-3}$  M. The parallel cathodic Tafel plots obtained in Figure 5 indicate that the hydrogen evolution is activation controlled and the reduction mechanism is not affected by the presence of inhibitor [18–21].

#### 4. Conclusion

The principal findings of present work can be summarized as follows:

1. A correlation was obtained between the percentage inhibition efficiencies calculated from the electrochemical measurements and weight loss data.
2. Steady state electrochemical measurements have shown that the studied inhibitor act as mixed inhibitor for the corrosion of steel in 1 M HCl without modifying the mechanism of hydrogen evolution reaction.
3. The adsorption of the 1,1'-(pyridine-2,6-dihylbis(methylene))bis(5-methyl-1-*H*-pyrazole-3-carboxylic acid) compounds on the mild steel surface in 1 M HCl obeys the Langmuir adsorption isotherm model.
4. The inhibitory efficiency is dependent of the concentration of the (EM1) compounds and the efficiency reaches 93% at  $10^{-3}$  M.

#### References

1. I. Lukovits, E. Kalman and F. Zucchi, *Corrosion (Houston)*, 2001, **57**, no. 1, 3.
2. G. Gunasekaran and L.R. Chauhan, *Electrochim. Acta*, 2004, **49**, 4387.
3. Y. ELouadi, F. Abridgach, A. Bouyanzer, R. Touzani, O. Riant, B. ElMahi, A. El Assyry, S. Radi, A. Zarrouk and B. Hammouti, “Corrosion inhibition of mild steel by new N-heterocyclic compound in 1 M HCl: Experimental and computational study,” *Der Pharma Chemica*, 2015, **7**, no. 8, 265.
4. M.E. Belghiti, A. Nahlé, A. Ansari, Y. Karzazi, S. Tighadouini, Y. El Ouadi, A. Dafali, B. Hammouti and S. Radi, “Inhibition effect of E and Z conformations of 2-pyridinealdazine on mild steel corrosion in phosphoric acid,” *Anti-Corros. Meth. Mater.*, 2017, **64**, no. 1, 23.
5. Y. Elouadi, F. Abridgach, A. Bouyanzer, R. Touzani, A. El Assyry, A. Zarrouk and B. Hammouti, “Theoretical and Experimental Studies on the Corrosion Inhibition

- Potentials of Two Tetrakis Pyrazole Derivatives for Mild Steel in 1.0 M HCl,” *Port. Electrochim. Acta*, 2017, **35**, no. 3, 159.
6. I. Merimi, Y. El Ouadi, K.R. Ansari, H. Oudda, B. Hammouti, M.A. Quraishi, F.F. Alblewi, N. Rezki, M.R. Aouad and M. Messali, “Adsorption and Corrosion Inhibition of Mild Steel by ((Z)-4-((2,4-dihydroxybenzylidene)amino)-5-methyl-2,4-dihydro-3H-1,2,4-triazole-3-thione) in 1 M HCl: Experimental and Computational Study,” *Anal. Bioanal. Electrochem.*, 2017, **9**, no. 5, 640.
  7. M. El Azzouzi, A. Aouniti, S. Tighadouin, H. Elmsellem, S. Radi, B. Hammouti, A. El Assyry, F. Bentiss and A. Zarrouk, “Some hydrazine derivatives as corrosion inhibitors for mild steel in 1.0 M HCl: Weight loss, electrochemical, SEM and theoretical studies,” *J. Mol. Liq.*, 2016, **221**, 633.
  8. C.A. Daoudi, B. Hammouti, T. Ben Hadda and M. Benkaddour, *Corros. Sci.*, 2006, **48**, 2987.
  9. Y. El Ouadi, A. Bouyanzer, L. Majidi, J. Paolini, J.-M. Desjobert, J. Costa, A. Chetouani, B. Hammouti, S. Jodeh, I. Warad, Y. Mabkhot and T. Ben Hadda, *Res. Chem. Intermed.*, 2015, **41**, 7125. doi: [10.1007/s11164-014-1802-7](https://doi.org/10.1007/s11164-014-1802-7)
  10. L. Herrage, B. Hammouti, S. Elkadiri, A. Aouniti, C. Jama, H. Vezin and F. Bentiss, *Corros. Sci.*, 2010, **52**, 3042.
  11. M.A. Quraishi, A. Singh and D.K. Yadav, *Mater. Chem. Phys.*, 2010, **122**, 114.
  12. C.H. Hsu and F. Mansfeld, *Corrosion*, 2001, **57**, 747.
  13. A. Popova and M. Christov, *Corros. Sci.*, 2006, **48**, 3208.
  14. T. Tsuru, S. Haruyama and B. Gijutsu, *J. Jpn. Soc. Corros. Eng.*, 1978, **27**, 573.
  15. E. McCafferty and N. Hackerman, *J. Electrochem. Soc.*, 1972, **119**, 146.
  16. J.M. Bastidas, J.L. Polo and E. Cano, *J. Appl. Electrochem.*, 2000, **30**, 1173.
  17. S. Muralidharan, M.A. Quraishi and V.K. Iyer, *Corros. Sci.*, 1995, **37**, 1739.
  18. I. Belfilali, A. Chetouani, B. Hammouti, A. Aouniti, S. Louhibi and S.S. Al-Deyab, *Int. J. Electrochem. Sci. Corrosion Science*, 2012, **7**, 3997.
  19. A. Rochdi, O. Kassou, N. Dkhireche, R. Tourir, M. El Bakri, M.E. Touhami, M. Sfaira, B. Mernari and B. Hammouti, *Corros. Sci.*, 2014, **80**, 442.
  20. H. Zarrok, A. Zarrouk, R. Salghi, B. Hammouti, M. Elbakri, M.E. Touhami, F. Bentiss and H. Oudda, *Res. Chem. Intermed.*, 2014, **40**, 801.
  21. R.S. Abdel Hameed and A.H. Shamroukh, *Int. J. Corros. Scale Inhib.*, 2017, **6**, no. 3, 333. doi: [10.17675/2305-6894-2017-6-3-8](https://doi.org/10.17675/2305-6894-2017-6-3-8)

